

14p

ATS-16601
NGR-39-007.011

THE USE OF COD AND PLASTIC INSTABILITY IN
CRACK PROPAGATION AND ARREST IN SHELLS

by

F. Erdogan and M. Ratwani

(NASA-CR-138625) THE USE OF COD AND
PLASTIC INSTABILITY IN CRACK PROPAGATION
AND ARREST IN SHELLS (Lehigh Univ.)
23 p HC \$4.25

CSCL 20K

G3/32 Unclass 16601

N74-27480

Lehigh University
Bethlehem, Pennsylvania
January 1974

PAPER 6

THE USE OF COD AND PLASTIC INSTABILITY IN CRACK PROPAGATION AND ARREST IN SHELLS

F. Erdogan

Professor of Mechanics, Lehigh University, Bethlehem, Pa.

M. Ratwani

Northrop Corp. Aircraft Division, Hawthorne, Calif.

Contents

1. Introduction
2. Elastic shell with a part-through crack
3. Part-through crack with fully-yielded net ligament
4. Fracture criterion based on plastic instability
5. Depressurization and crack arrest

Summary

This paper deals with the initiation, growth, and possible arrest of fracture in cylindrical shells containing initial defects. For those defects which may be approximated by a part-through semi-elliptic surface crack which is sufficiently shallow so that part of the net ligament in the plane of the crack is still elastic, the existing flat plate solution is modified to take into account the shell curvature effect as well as the effect of the thickness and the small scale plastic deformations. The problem of large defects is then considered under the assumptions that the defect may be approximated by a relatively deep meridional part-through surface crack and the net ligament through the shell wall is fully yielded. The results given in the paper are based on an 8th order bending theory of shallow shells using a conventional plastic strip model to account for the plastic deformations around the crack border.

For shells with shallow surface cracks the plasticity corrected stress intensity factor given in Section 2 of this paper may be used to study the phenomena such as plane strain fracture, fatigue crack propagation, and stress corrosion cracking. To study the fracture problem in shells containing large defects in Section 3 the results of COD calculations are presented. These results may be used in conjunction with either a critical crack opening stretch type fracture criterion, or a plastic instability criterion which is described in Section 4. This section also contains a comparison of the calculated results with those obtained from the experiments on steel pipes.

In Section 5 a preliminary attempt is made to come to grips with the important problem of dynamics of crack propagation in pressurized shells which is coupled with the problem of fluid mechanics. As an example, the initial stage of crack propagation in a finite volume container is considered. The results indicate that in some cases the fracture arrest may be possible due to depressurization.

List of Symbols

A	:	Area of crack opening (orifice).
A_m, A_b	:	Membrane and bending components of the stress intensity factor ratio in shells.
2a	:	Crack length.
COD	:	Crack opening displacement.
d	:	Depth of the surface crack.
$d_1 =$:	$4a\sigma_Y/E$: normalizing factor for δ .
E	:	Young's modulus.
h	:	Shell thickness.
K	:	Stress intensity factors.
N_o	:	Membrane load in circumferential direction.
p_o	:	Pressure.
R	:	Shell radius of curvature.
δ	:	Crack opening displacement or stretch.
$\lambda =$:	$[12(1-\nu^2)]^{1/4} a / (Rh)^{1/2}$: shell parameter.
σ_Y	:	Yield strength.
$\bar{\sigma}$:	Flow stress.

1. Introduction

Generally, in pipes, pressure vessels, and a great variety of other plate and shell structures the main cause of structural failure appears to be the nucleation and the growth of cracks from an existing dominant imperfection or flaw which is usually a surface or an internal defect of arbitrary shape and orientation. In some cases inspection and nondestructive testing procedures may provide a fairly good estimate of the size, shape, orientation, and location of the dominant defect. However, in most analysis relating to the reliability and integrity of the structure, generally one simply conjectures the existence of such defects and proceeds with the application of a relevant fracture criterion. Similar to all failure studies, the work leading to the application of the fracture criterion has three different components which may initially be considered independently. These are:

(a) The experimental determination of the "characteristic strength parameter" representing the inherent resistance of the material to fracture corresponding to the conjectured mode of fracture.

(b) The solution of the mechanics problem for the given geometry and the external loads in order to determine the "critical load factor" representing the severity of the applied loads.

(c) Development of an appropriate fracture theory and a related quantitative "fracture criterion". This is usually

nothing but the direct comparison of the "characteristic strength parameter" of the material with the "critical load factor". It is clear that in fracture studies the development of the fracture theory and selection of a proper fracture criterion must precede the experimental determination of the characteristic strength parameters and the theoretical evaluation of the corresponding critical load factors.

In shell structures, including the pipes and pressure vessels, if the flaw geometry and the external loads are such that the stress state in the medium is basically elastic and the plastic and other inelastic deformations are restricted to the relatively small toroidal region enclosing the crack periphery, the ensuing fracture is generally of plane strain type and may be classified as "low energy" type. Consequently, the "fracture toughness" G_{IC} (or the corresponding "critical stress intensity factor" K_{IC}), the fatigue crack propagation constants, the corrosion cracking threshold value of the stress intensity factor K_{ISCC} , and similar quantities may be considered as the material parameters representing the resistance of the structure to failure. In this case the appropriate "load factor" is the stress intensity factor K (or quantities which may readily be evaluated in terms of K), and hence in fracture studies it is sufficient to perform a linear analysis.

On the other hand, if the crack geometry, the external loads, and the environmental conditions are such that there are large scale plastic deformations around the crack front, the resulting fracture will be of "high energy" type. In this case one relevant criterion which lends itself reasonably well to standardization and analytical treatment is that of the "critical crack opening stretch" δ_c . The criterion appears to work rather successfully for "plane stress" type fracture of thin sheets with relatively large plastic zones around the crack.

The calculated results for the crack opening displacement (COD) in shells indicate that for a given shell geometry COD is a monotonically increasing function of the hoop stress $\sigma_{\theta\theta}$ with a slope which also increases quite rapidly for increasing values of $\sigma_{\theta\theta}/\sigma_Y$, σ_Y being the yield strength. This suggests that around a certain value of the hoop stress, any small increase in the applied load may cause a considerable increase in COD, resulting in, what may be called, "the plastic instability" of the material ahead of the crack and causing rupture. Thus, the basis of another fracture criterion to be used in studying the rupture of thin sheet structures may be the concept of plastic instability which may quantitatively be characterized in terms of a standard slope in the COD vs $\sigma_{\theta\theta}$ relationship.

The primary objective of this paper is to provide the necessary analytical tools for the application of different types of fracture criteria mentioned above to the shell structures. Of particular interest will be the problem of fracture propagation and arrest in a cylindrical shell containing an initial surface flaw. It will be assumed that the flaw has the most unfavorable geometry and orientation, namely it is a crack lying on a meridional plane. First we will consider the problem of a part-through

crack for which either the crack depth-to-shell thickness ratio d/h is sufficiently small or the external loads (and/or the temperature) are sufficiently low so that the plastic deformations are confined to the neighborhood of the crack border and the stress state in the shell is basically elastic. The main analytical problem here is the evaluation of the (plasticity-corrected) stress intensity factor along the crack front.

We will then consider the problem of a relatively deep surface crack or a relatively large internal crack for which the net ligament in the plane of the crack is fully yielded (Figures 1b and 2). In this case it will be assumed that the plastic deformations are also spread around the crack ends through the entire wall thickness. Here the main analytical problem is the evaluation of the crack opening stretch at the locations of expected fracture propagation. Calculated COD values will be compared with the experimental results obtained by Fearnough and Watkins¹, and by Cowan and Langford². The results of the burst tests performed by Anderson and Sullivan³, will be used to test the validity of the critical crack opening stretch as the fracture criterion. To study the effectiveness of the concept of "plastic instability" as a correlation tool in "plane stress" type fracture, the calculated results will be compared with the experimental results obtained by Kiefner, et al.⁴ Finally, the problem of the rupture of the net ligament and the ensuing crack propagation and arrest in a pressurized cylinder of finite volume will be considered theoretically.

2. Elastic Shell with a Part-Through Crack

The elasticity solution of the part-through crack problem in plates or shells is not yet available. For plates there are some approximate solutions which are believed to give reasonably accurate results under some simplifying assumptions regarding the crack geometry and the boundary layer effect. These solutions (which are reviewed in the ASME volume on The Surface Crack⁵) are essentially based on the modification of the elliptic crack problem considered by Green and Sneddon⁶. A brief review of these results with further modification taking into account the shell curvature effect may be found in the paper by Erdogan and Ratwani⁷. In this paper only the expression for the stress intensity factor in a cylindrical shell will be repeated.

Consider the crack geometry shown in Figure 1b. Let us assume that the crack depth-to-thickness ratio d/h , the applied load level, and the ambient temperature are such that the main bulk of the shell cross-section is elastically deformed, and the plastic deformations are restricted to a relatively small region along the crack border. The (plasticity-corrected) stress intensity factor along the crack front may then be approximated by

$$K(\phi) = \frac{N_o}{h} \sqrt{\pi d} \frac{c_t c_c}{Q} \left(\frac{d^2}{a^2} \cos^2 \phi + \sin^2 \phi \right)^{1/4} \quad (1)$$

where

ϕ is the angular parameter measured from the x-axis (see Figure 2) which defines the leading edge of the crack through the following parametric equations:

$$x = a \cos \phi, \quad z = -d \sin \phi, \quad (2)$$

N_o/h is the hoop stress acting on the shell outside the perturbation zone of the crack,

d, a, h are the dimensions shown in Figure 1a,

$$Q = [E^2(k) - 0.212 \frac{N_o^2}{h^2 \sigma_y^2}]^{1/2}, \quad (3)$$

$E(k)$, ($k^2 = 1 - d^2/a^2$) is the complete elliptic integral of the second kind,

σ_y is the yield strength of the material,

$$c_t = \frac{1 + 0.122(1 - d/2a)^2}{[1 - (d/a)^4]^{1/2}}, \quad (d < a), \quad (4)$$

$$c_c = (A_m - 1) \frac{d}{h} + 1, \quad (5)$$

$$A_m = 0.481\lambda + 0.614 + 0.386e^{-1.25\lambda}, \quad (6)$$

$$\lambda = [12(1-\nu^2)]^{1/4} \frac{a}{(Rh)^{1/2}}, \quad (7)$$

R being the (mean) radius of curvature of the cylindrical shell.

In this analysis Q accounts for the plasticity correction, c_t is the thickness correction factor, c_c is the shell curvature correction factor with A_m being the stress intensity factor ratio in the shell with a through crack.

3. Part-Through Crack with Fully-Yielded Net Ligament

In this section a brief description of the results regarding the part-through surface crack in a cylindrical shell with fully-yielded net ligament will be presented. As shown in Figure 2a the geometry of the internal defect is generally quite irregular, and in a given "defect zone" there may be more than one internal crack. Here we will assume that the total defect zone may be replaced by a single part-through crack of equivalent size and orientation, and of idealized shape (Figure 2b). Further, it will be assumed that the net ligaments connecting the idealized crack to the inner and the outer surfaces of the shell are fully yielded and carry only membrane stresses of magnitude σ_y , the yield strength of the material (Figure 2c). Finally, it will be assumed that the plastic deformations have been spread beyond the ends of the crack up to a distance p (Figure 2b) and the plastic region may be approximated by a plastic strip similar to that in the Barenblatt-Dugdale model. The plastic strip in the yield

zone $a < x < a+p = a_p$ is assumed to carry a membrane load $N_{yy} = N$ and a moment resultant $M_{yy} = M$ where N and M are as yet unknown and x, y, z are the rectangular coordinates in axial, tangential, and radial directions. The main objective of the analysis is the determination of the crack opening stretch along the crack boundary.

The method of solution and extensive computed results regarding the stress intensity factor and the COD in cylindrical shells were presented in the previous work of Erdogan and Ratwani^{8,9,7}. In this paper we will repeat some of the relevant results from the previous work and present some new results on the application of the plastic instability concept.

Calculated results for the crack opening stretch δ are shown in Figures 3-9. Figure 3 shows the crack opening displacement δ_0 in the neutral surface of the shell at the mid-section of the crack ($x=0, z=0$) for a through crack. In this and in the subsequent figures the normalizing factor for COD is defined by

$$d_1 = 4a\sigma_y/E, \quad (8)$$

where E is the Young's modulus. Figure 4 shows the conventional crack opening stretch δ evaluated in the neutral surface of the shell at the (actual) crack tip ($x=a, z=0$). Figures 3 and 4 clearly indicate the influence of the shell curvature (as represented by the shell parameter λ defined by equation (7)) on the crack opening displacement. In Figures 5-8 δ^t is the crack opening stretch (which includes curvature and bulging as well as the membrane effects) at the leading edge of the crack in the mid-section ($x=0, z = h/2 - d$) for a cylindrical shell with an external part-through crack of depth d . The figures essentially show the load carrying capacity of the shell for a constant crack opening stretch $\delta^t = \delta_c$. In these figures the small circles shown for $d=h$ for various values of δ/d_1 correspond to the load levels $N_0/h\sigma_y$ giving these COD values at the crack tip $x=a$ in the shell having a through crack of the same length $2a$. Generally the extrapolated values of the load $N_0/h\sigma_y$ for constant δ^t curves at $d=h$ are lower than the load corresponding to the same COD at the crack tip in the through crack case. This means that, if the critical COD criterion is valid, at least theoretically it is possible to have leak before burst (or before any additional crack extension).

The load carrying capacity for the shell with a through crack is shown in Figure 9. Here λ represents the crack length (see equation (7)), and δ is calculated at $x=a$.

Figures 10 and 11 show a comparison of experimentally measured COD values in zircaloy pressure tubes used in steam generating heavy water reactors (Fearnehough and Watkins¹, and Cowan and Langford²) with those calculated by using the same dimensions and the same material constants (see Erdogan and Ratwani⁹ for details). Generally the agreement appears to be quite satisfactory. Figure 12 shows the correlation of the results of the burst tests performed by Anderson and Sullivan³ on 2014-T6 aluminum cylinders. In these figures the open circles correspond to

the elastic stress intensity factor in the shell given by

$$K = (A_m + A_b) (p_o R/h) (\pi a_c)^{1/2} \quad (9)$$

where A_m and A_b , respectively, are the membrane and bending components of the stress intensity factor ratio in a cylindrical shell with a through crack, p_o is the burst pressure and a_c is the value of a at burst. K_{pl} is the plasticity corrected K obtained from (9) by replacing a_c by $a_c + p$, p being the plastic zone size computed from the plastic strip model. The figure indicates that, for the material under consideration, compared to $K = \text{constant}$, or $K_{pl} = \text{constant}$, $\delta = \delta_c = \text{constant}$ appears to be a better rupture criterion.

4. Fracture Criterion Based on Plastic Instability

From Figures 3 and 4 and from the similar results given for the part-through crack in a cylindrical shell by Erdogan and Ratwani⁷ it is easy to observe that for a shell with a given crack geometry in the neighborhood of a certain value of the applied load $N_o/h\sigma_y$ any small increase in N_o may cause a very large increase in the COD (δ or δ^t). This simply means that about this particular applied load the phenomenon which takes place at the leading edge of the crack is similar to the necking phenomenon observed in a ductile tensile bar, that is, the material is subjected to plastic instability. Moreover, the slopes of δ/d_1 vs $N_o/h\sigma_y$ curves increase so rapidly with increasing N_o that the load corresponding to the plastic instability may be determined from these figures within an acceptable degree of accuracy by assuming a hypothetically selected high slope (such as 20). Once a critical (standard) slope (in δ vs N_o curves) is selected, the load carrying capacity of the shell (N_o vs λ) may then be obtained from Figure 4 for the through crack and from the similar figures for the part-through crack. These theoretical results are shown in Figure 13 where a slope of 20 in δ/d_1 vs $N_o/h\sigma_y$ curves was used to determine the plastic instability load N_o for a given λ and d/h . In this and in some of the subsequent figures the notation $\bar{\sigma}$ rather than σ_y is used. As suggested by Kiefner, et al.⁴, in this type of analysis it is more appropriate to use a "flow stress" $\bar{\sigma}$ rather than the standard 0.2% offset yield strength σ_y , $\bar{\sigma}$ being somewhat higher than σ_y . $\bar{\sigma}$ may be selected as (a) $\bar{\sigma} = (1+\alpha)\sigma_y$, α being a fixed percentage, or (b) $\bar{\sigma} = (\sigma_y + \sigma_u)/2$, σ_u being the ultimate strength, or (c) $\bar{\sigma} = \sigma_y + \Delta\sigma_y$, $\Delta\sigma_y$ being a constant (taken as 10,000 psi by Kiefner, et al.⁴ for pipe steels they tested). Needless to say, the theoretical results given by Figure 13 are not affected by any particular selection of $\bar{\sigma}$.

Figures 14 and 15 show the comparison of the theoretical and experimental results. The experiments were performed by Kiefner, et al.⁴ on steel pipes (X52, X60V, X65C, X60C) containing a through crack. In these figures the experimental results were normalized by selecting $\bar{\sigma} = \sigma_y + 10,000$ psi as suggested by the Authors. A comparison of some of the experimental results given by Kiefner, et al.⁴ for the part-through crack in steel pipes (X52, X60C, X60V) and the theoretical results shown in

Figure 13 is given in Figures 16-18. In these figures the theoretical curve is for $d/h=0.5$; the experimental results were obtained for $0.492 < d/h < 0.511$. The figures show the comparison for three values of α , $\alpha=0$, $\alpha=0.05$, $\alpha=0.10$ in $\bar{\sigma} = \sigma_y(1+\alpha)$.

From Figures 14-18 it may be seen that the concept of plastic instability appears to be rather effective in correlating the results of the rupture tests. The figures also indicate that in the type of analysis which is based on an elastic-perfectly-plastic strip model, some increase in the yield strength (to a value called flow stress) is necessary. It should be pointed out that even though the critical crack opening stretch criterion gave rather good results for aluminum and titanium cylinders (see Figure 12 and the work of Erdogan and Ratwani⁹), it was not satisfactory for steel cylinders*.

5. Depressurization and Crack Arrest

In pressurized pipes, containers, and other shell structures, generally the first phase of fracture is the rupture of the net ligament around a defect zone shown in Figure 2 through any one or a combination of fracture mechanisms. This formation of a through crack will be followed by depressurization. The ensuing phenomenon leads to a coupled fracture dynamics - fluid mechanics problem which is rather difficult to formulate. It is worthwhile, however, to mention two idealized cases for which it may be possible to construct approximate models.

The first refers to an infinitely long cylindrical shell containing pressurized gas. If the velocity of sound in the gas is smaller than the terminal velocity of the crack in the shell (which is usually the case), and if after the formation of the through crack the initial acceleration phase of the crack propagation is of sufficiently short duration, then it is possible for the crack to grow at a constant velocity driven by a constant pressure (which is the initial pressure). In this "steady-state" case the elastic energy released by the shell and the expanding gas will be spent largely as kinetic energy (for the unfolding shell walls and for the gas), plastic work, and fracture energy, the energy balance equation determining the crack velocity. Because of the geometry of the medium, the stress waves generated along the crack path in the shell will interfere with the main membrane loads after traveling around the shell circumference. Hence, even in this "steady-state" crack propagation a certain amount of waviness in the crack path would be expected. If the driving force is sufficiently high, it may not be possible to maintain a steady longitudinal crack path, and the crack will keep branching to absorb the excess energy**. On the other hand,

* The explanation of the success or failure of the two criteria in their application to the two groups of materials under consideration may perhaps lie in the differences in the nature of the plastic deformations and in the shape of the yield zones around the crack tip.

**The natural waviness of the crack path and the material imperfections will also increase the tendency of the crack to branch or deviate from a meridional path.

if the driving force is not high enough, the crack velocity corresponding to the energy balance may be less than the sound velocity in the gas. In this case the "steady state" crack propagation cannot take place and as a result of depressurization the crack would eventually be arrested.

The second problem refers to the fracture of a finite volume cylindrical container. In this case one may consider the problem as being quasi-static. The justification of this assumption is based on the fact that the part of the phenomenon which is of primary interest here is the initial stage for which the crack velocity and as a result the inertia effects are relatively small, and the distortion in the overall geometry of the shell is negligible (meaning that the existing shell solution is still valid). If this phase of the study leads to the conclusion that the fracture will not be arrested and will continue with increasing velocity and overall distortion, the inertia effects may indeed not be negligible. However, in this case the failure is very likely to be catastrophic and the solution, even if it can be obtained, is of little practical interest.

The propagation and arrest of a crack in a finite volume container will now be considered under the following additional assumptions:

(a) The medium in the container behaves either as a perfect gas or as a nonviscous liquid.

(b) The pressure drop in the container is assumed to be sufficiently "slow" so that the fluid mechanics problem may be treated as "one-dimensional" with the basic variables p (pressure), ρ (density), and v (discharge velocity).

(c) The "orifice" may be approximated by an ellipse with the axes $2a$ (the crack length) and δ_0 (the COD at $x=0$).

(d) The last assumption concerns the dynamic rupture criterion or some statement about the motion of the crack which provides one of the two basic equations for the solution of the problem. Very little is known quantitatively about the velocity-dependence of the fracture resistance parameters such as K_{IC} or δ_c aside from the fact that they are sensitive to the crack velocity as well as to the temperature. Therefore in the model that follows it will simply be assumed that after the rupture of the net ligament the crack will grow either with a constant velocity or with a constant acceleration. However, the analysis is such that one may postulate any function for the crack length, $2a(t)$.

Within the confines of these assumptions, the basic variables of the problem are $p(t)$ (pressure), $\rho(t)$ (density), $v(t)$ (discharge velocity), and $a(t)$ (the half-crack length). The relevant equations to determine these functions are:

- (i) $pp^{-\gamma} = \text{constant}$ (adiabatically expanding gas), or
 $pp^{-1} = \text{constant}$ (isothermally expanding liquid),

(ii) The energy equation which may be expressed as (see Landau and Lifshitz¹⁰)

$$v = \left(\frac{2\gamma}{\gamma-1} \frac{p}{\rho} \right)^{1/2} \text{ (gas), } v = [2(p-p_e)/\rho_e]^{1/2} \text{ (liquid).} \quad (10)$$

(iii) The continuity equation

$$\tau dp = - \Omega A(t) \rho_e v(t) dt \quad (11)$$

where τ is the volume of the container, Ω is a discharge shape factor, $A(t)$ is the area of the "orifice", and ρ_e is the density at the "exit". From the shell solution A may be approximated by

$$A(t) = \pi a^2 p \left(\frac{2R}{hE} + \frac{1.47a^2}{h^2E} \right). \quad (12)$$

(iv) Motion of the crack

$$a(t) = a_0 + v_c t \text{ (constant velocity),} \quad (13)$$

$$a(t) = a_0 + \frac{1}{2} b t^2 \text{ (constant acceleration),} \quad (14)$$

or any given function.

Solving these equations for a constant velocity crack in a gas-filled container we find

$$p(a) = \left\{ p_0^{-\alpha} + \frac{\pi \alpha C}{hE v_c} \left[\frac{2R}{3} (a^3 - a_0^3) + \frac{1.47}{5h} (a^5 - a_0^5) \right] \right\}^{-1/\alpha}, \quad (15)$$

$$C = \frac{\Omega \gamma}{\tau} \sqrt{\frac{2\gamma}{(\gamma-1)\rho(0)}} p_0^{1/2\gamma} p_e^{1/\gamma}, \quad \alpha = \frac{3(\gamma-1)}{2\gamma},$$

where p_0 is the initial pressure, $p_0 = p(a_0)$.

Similarly for a constant acceleration crack we obtain

$$p(a) = [p_0^{-\alpha} + \alpha K f(a)]^{-1/\alpha}, \quad (16)$$

$$K = \frac{1.47 \pi C}{h^2 E \sqrt{2b}}, \quad b_1 = \frac{2Rh}{1.47},$$

$$f(a) = \frac{1}{4.5} (a - a_0)^{4.5} + \frac{4a_0}{3.5} (a - a_0)^{3.5} + \frac{b_1 + 6a_0^2}{2.5} (a - a_0)^{2.5} \\ + \frac{2a_0(b_1 + 2a_0^2)}{1.5} (a - a_0)^{1.5} + 2a_0^2(b_1 + a_0^2) (a - a_0)^{0.5}.$$

Similarly for a container filled with a nonviscous liquid under isothermal conditions and for a constant velocity crack we obtain

$$p(a) - p_e = \{ (p_o - p_e)^{-1/2} + \frac{\pi \Omega p_e}{E h v_c} \sqrt{\frac{2}{\rho_e}} \left[\frac{2R}{3} (a^3 - a_o^3) + \frac{1.47}{5h} (a^5 - a_o^5) \right] \}^{-2}. \quad (17)$$

An expression similar to (16) may be obtained for a constant acceleration crack.

Figure 19 shows qualitatively the variation of pressure for a constant velocity crack ($\dot{a} = \text{constant}$), for a constant acceleration crack ($\ddot{a} = \text{constant}$), and that corresponding to a constant crack opening stretch $\delta = \delta_c$ as a function of the crack length (see Figure 9). $\delta = \delta_c$ represents the resistance of the shell whereas the depressurization curves $\dot{a} = \text{constant}$ or $\ddot{a} = \text{constant}$ represent the external loads. When the depressurization curve falls below the resistance curve the crack will be arrested. The main feature of the depressurization curves is that the possibility of crack arrest increases with increasing δ_c and decreasing crack velocity v_c or crack acceleration b .

Figure 20 shows a sample quantitative example for a constant velocity crack. In the figure the solid line corresponds to the static resistance curve $(\delta_c/d_1) = 2$. $p_y = \sigma_y h/R$ is the pressure corresponding to fully yielded shell. The net ligament may break through at a pressure lower than that which would initiate static fracture at the tip of a through crack of length $2a$. The drop in the resistance curve (dashed line) shown in the figure is assumed to account for the dynamic effects. Hence, when the net ligament ruptures, the input pressure p_o will generally be somewhat higher than the resistance (or equilibrium) value and the crack will start or continue to grow. The information used in the problem is: $\sigma_y = 70,000$ psi, $p_o = 434$ psi, $a_o = 1$ in., $\delta_c = 2d_1$, $h = 0.1$ in., $R = 10$ in., $l = 20$ in. (length of the container), $E = 10^7$ psi, $\gamma = 1.4$, $p_e = 14.7$ psi, $v_c = 5$ in./sec., $\Omega = 0.3$ (for air), $\Omega = 0.4$ (for water). $a = a_r$ shown in the figure corresponds to the arrest value of the crack length in the liquid-filled container. The figure indicates that even for a very slow crack velocity assumed in the solution, for an expanding gas the crack arrest (before the fracture reaches catastrophic proportions) does not seem to be possible. However, for expanding liquids the crack arrest during the initial stage of crack propagation appears to be quite possible.

In the foregoing example the critical crack opening stretch was used as the fracture criterion. It should however be noted that the problem could be solved by using the concept of plastic instability or any other fracture criterion and by assuming a more general function $a(t)$ for the length of the propagating crack.

Acknowledgment

This work was supported by NASA Langley Research Center under the Grant NGR-39-007-011 and Battelle Memorial Institute, Columbus, Ohio.

References

1. Fearnehough G D and Watkins B. Application of crack opening displacement approach to prediction of pressurized tube failure. *Int. J. Fracture Mechanics*, Vol 4, 1968, p 233.
2. Cowan A and Langford W J. Effect of hydrogen and neutron irradiation on the failure of flawed zircaloy 2 pressure tubes. *J. Nucl. Mat.*, Vol 30, 1969, p 271.
3. Anderson R B and Sullivan T L. Fracture mechanics of through-cracked cylindrical pressure vessels. NASA TN D-3252, 1966.
4. Kiefner J F, Maxey W A, Eiber R J and Duffy A R. The failure stress levels of flaws in pressurized cylinders. Paper presented at ASTM Sixth National Symposium on Fracture Mechanics, August 1972.
5. Swedlow J L (ed.). The Surface Crack: Physical Problems and Computational Solutions. ASME, 1972.
6. Green A E and Sneddon I N. The distribution of stress in the neighborhood of a flat elliptical crack in an elastic solid. *Proc. Cambridge Phil. Soc.*, Vol 46, 1950, p 159.
7. Erdogan F and Ratwani M. Fracture initiation and propagation in a cylindrical shell containing an initial surface flaw. *Nuclear Engineering and Design*, Vol 22, 1974 (to appear).
8. Erdogan F and Ratwani M. Plasticity and the crack opening displacement in shells. *Int. J. Fracture Mechanics*, Vol 8, 1972, p 413.
9. Erdogan F and Ratwani M. Fracture of cylindrical and spherical shells containing a crack. *Nuclear Engineering and Design*, Vol 20, 1972, p 265.
10. Landau L D and Lifshitz E M. Fluid Mechanics. Addison-Wesley, 1959.

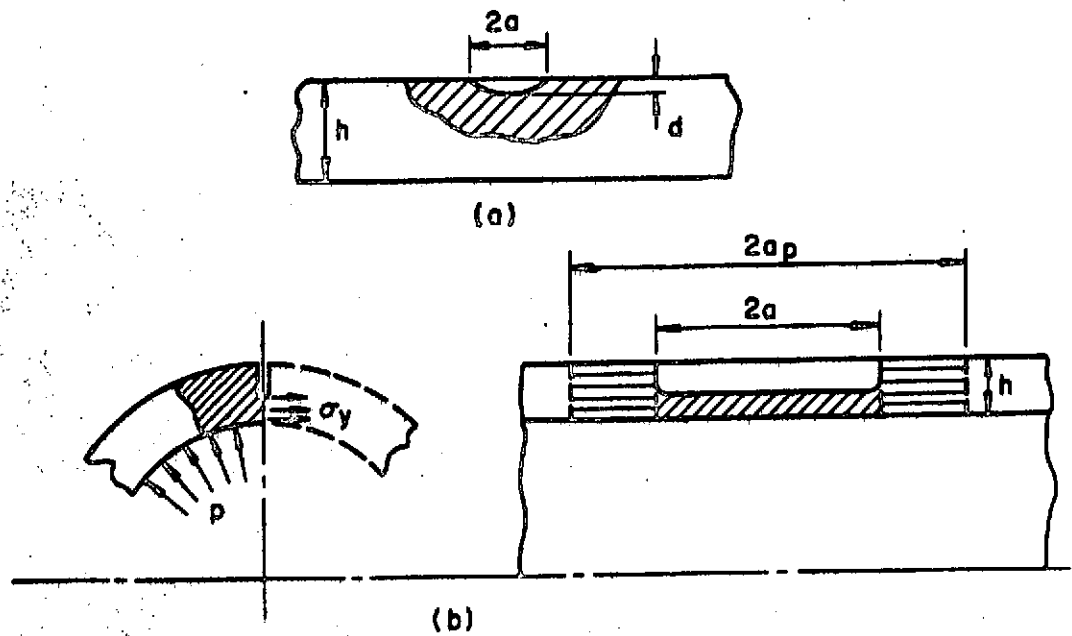


Fig. 1. Part-through crack geometries.

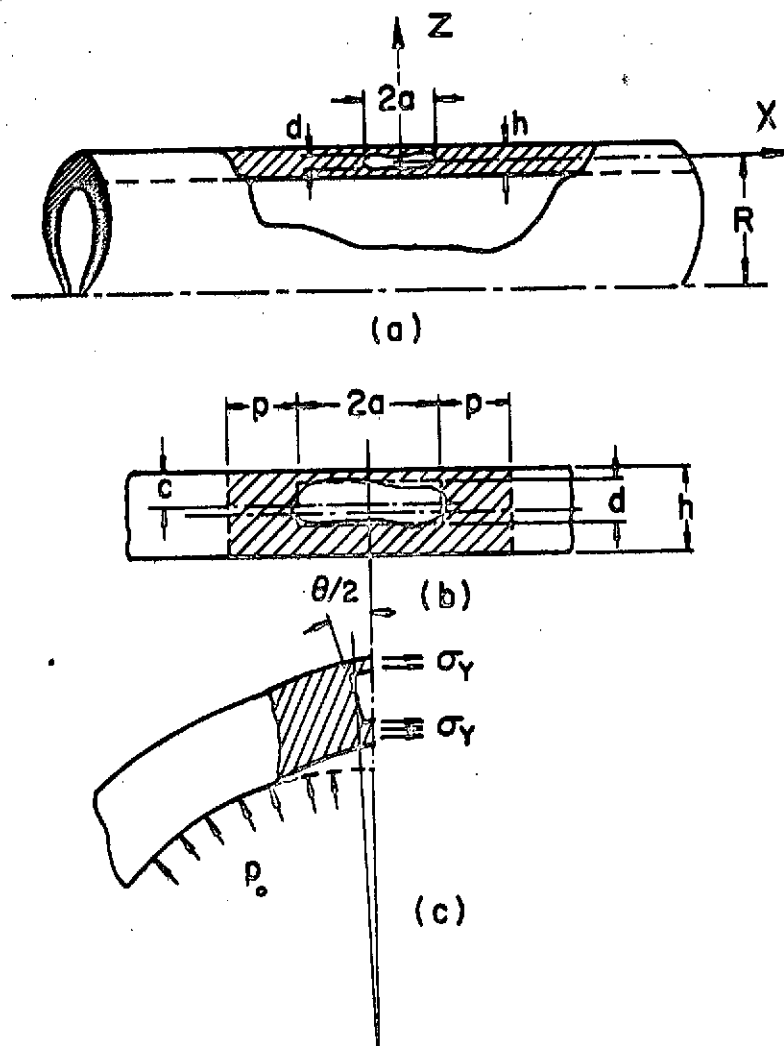


Fig. 2. Internal flaw in the shell with fully-yielded net ligaments.

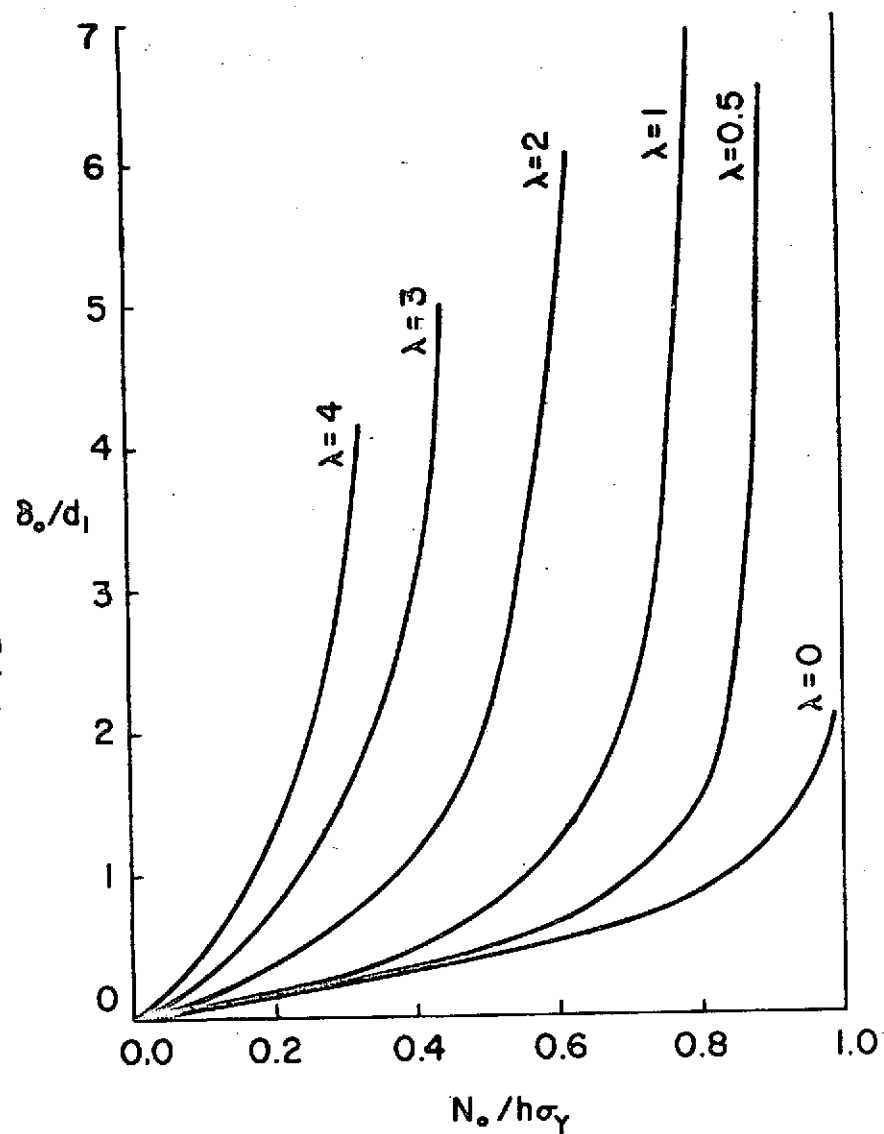


Fig. 3. Crack opening displacement in the neutral surface of the shell and at the mid-section of the crack ($x=0, z=0$).

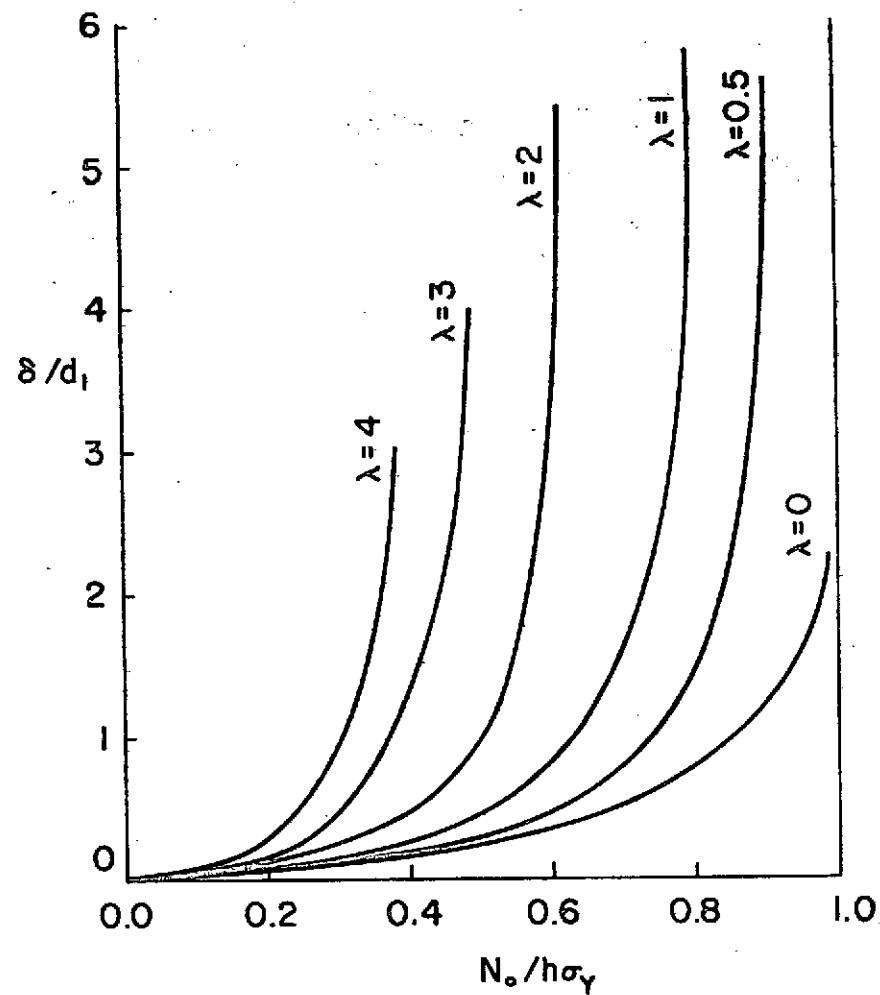


Fig. 4. Crack opening stretch in the neutral surface and at the crack tip ($x=a, z=0$).

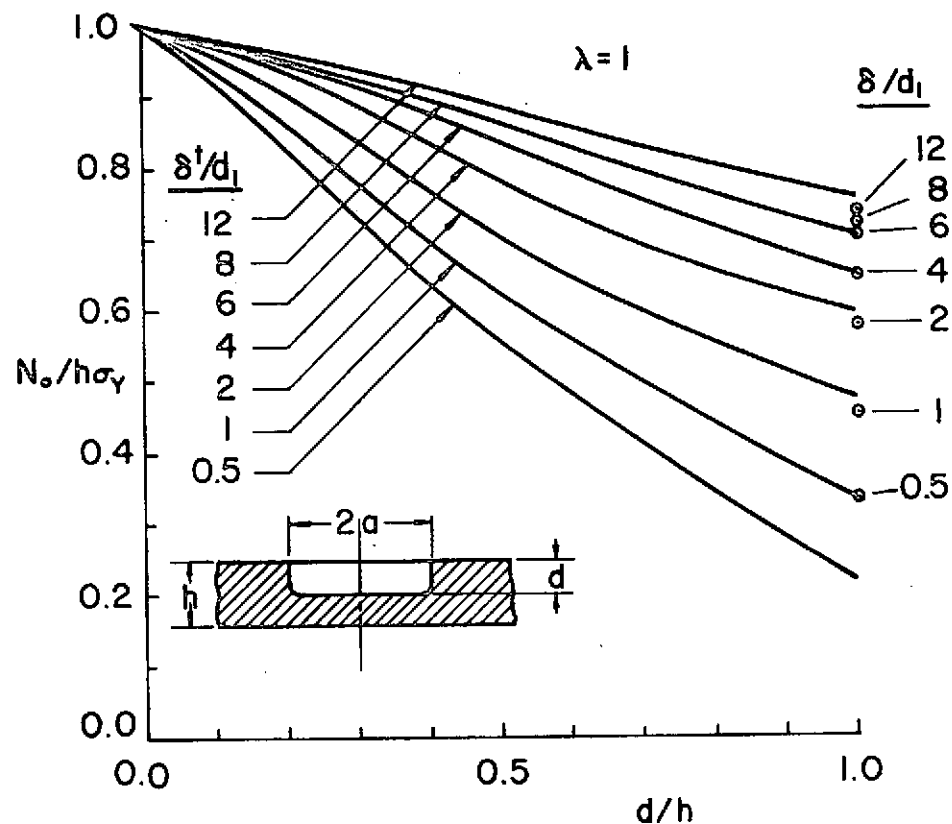


Fig. 5. N_0 vs. d for constant total crack opening stretch, δ_t at the leading edge of the crack in the mid-section ($x=0$, $z=h/2-d$) in a cylindrical shell with an external surface crack, $\lambda=1$.

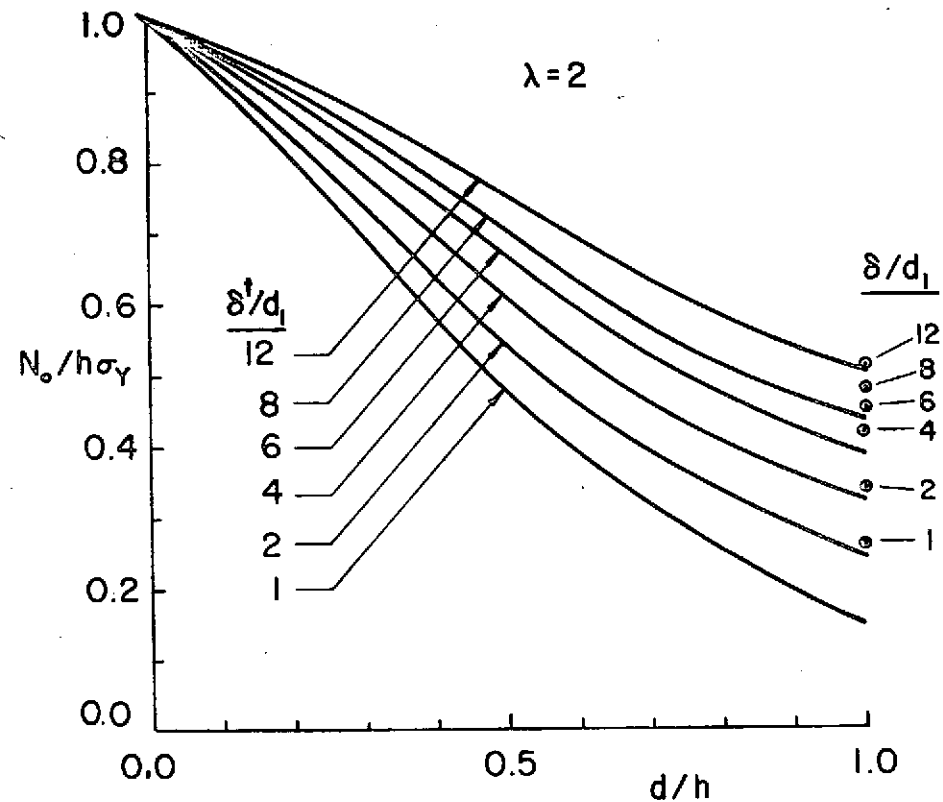


Fig. 6. N_0 vs. d for constant total crack opening stretch, δ_t at the leading edge of the crack in the mid-section ($x=0$, $z=h/2-d$) in a cylindrical shell with an external surface crack, $\lambda=2$.

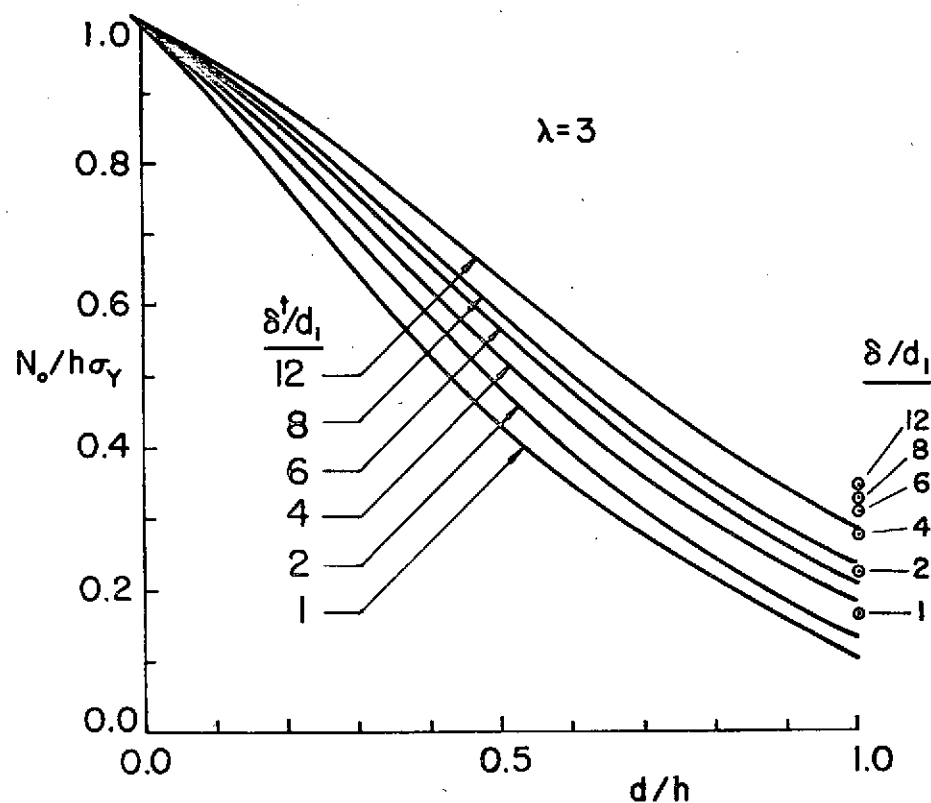


Fig. 7. N_0 vs. d for constant total crack opening stretch, δ_t at the leading edge of the crack in the mid-section ($x=0$, $z=h/2-d$) in a cylindrical shell with an external surface crack, $\lambda=3$.

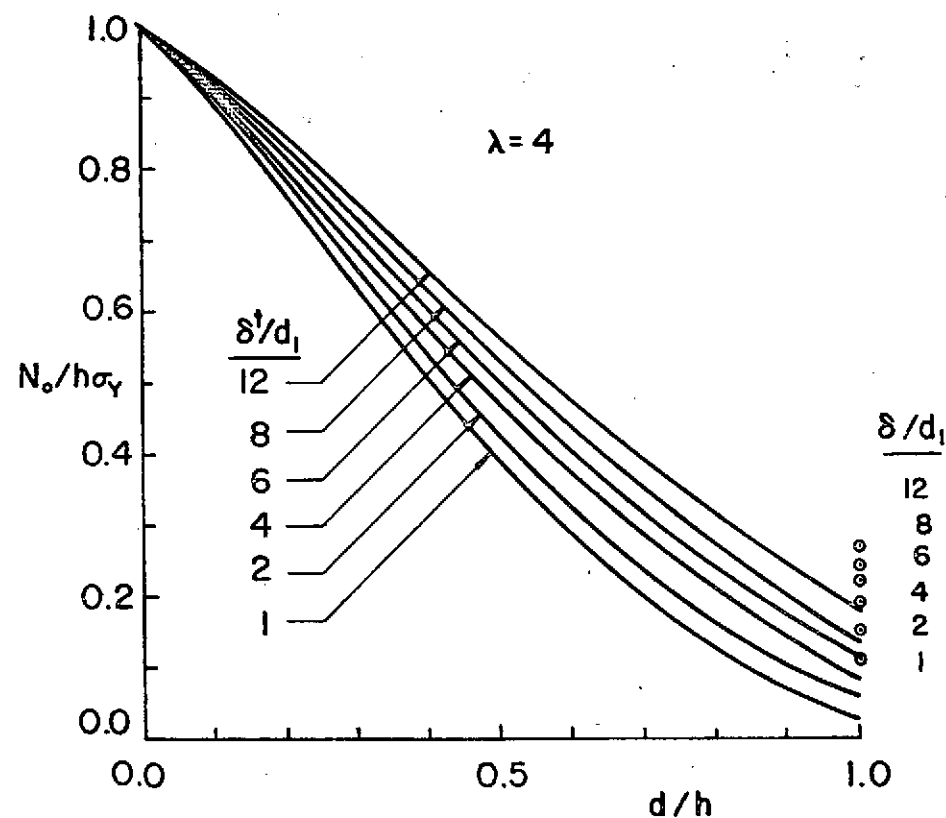


Fig. 8. N_0 vs. d for constant total crack opening stretch, δ_t at the leading edge of the crack in the mid-section ($x=0$, $z=h/2-d$) in a cylindrical shell with an external surface crack, $\lambda=4$.

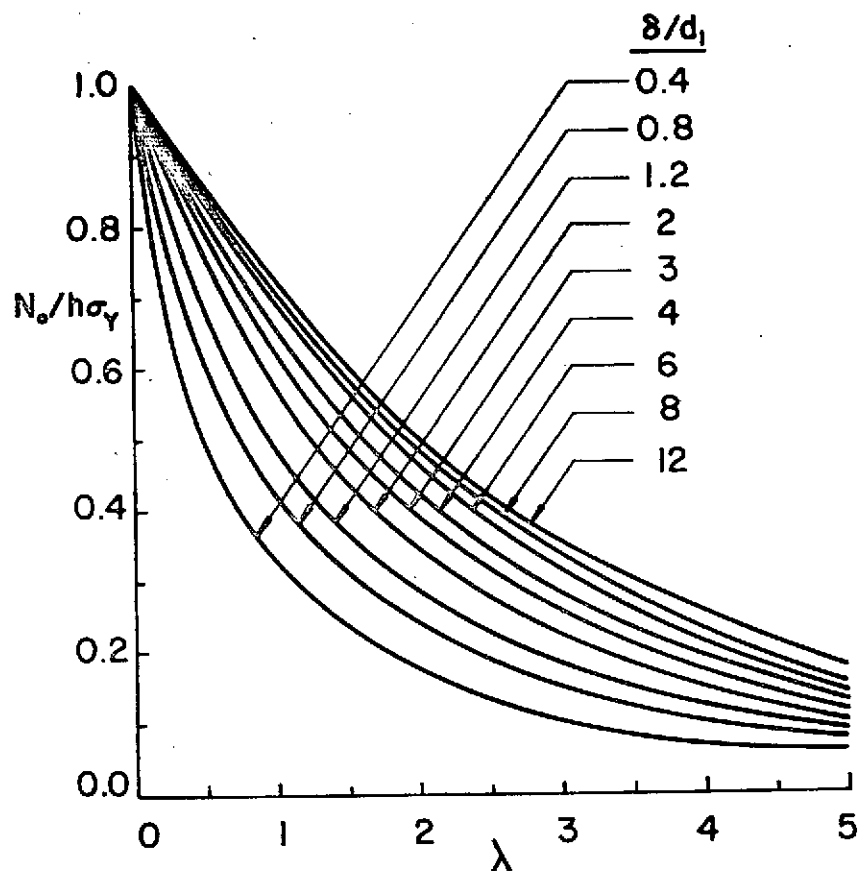


Fig. 9. N_o vs. λ for a constant crack opening stretch δ at the crack tip $x=a$ in a cylindrical shell containing a through crack.

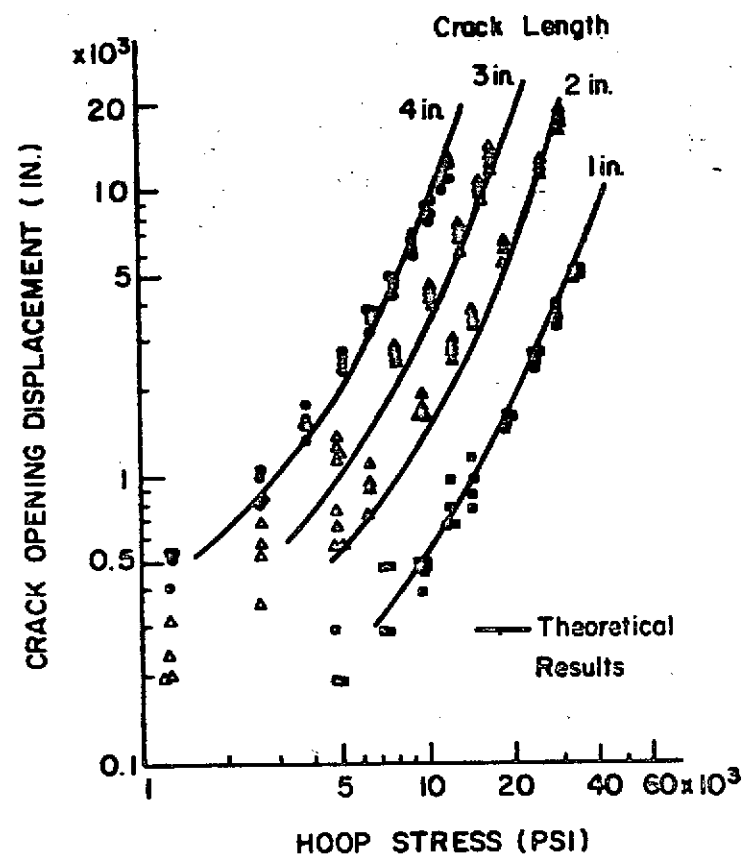


Fig. 10. Comparison of the calculated COD values with the experimental measurements of Fearnough and Watkins (1968).

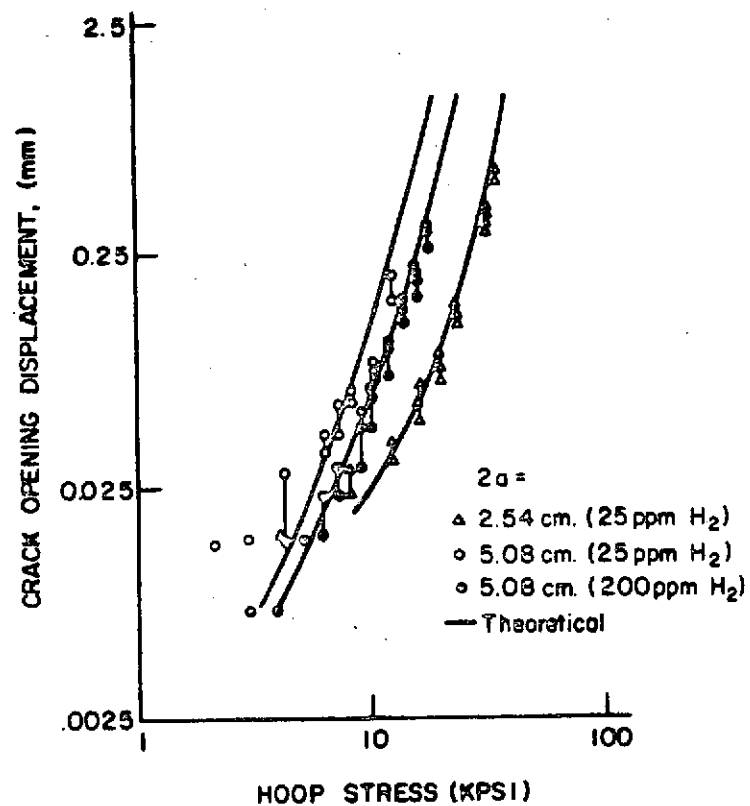


Fig. 11. Comparison of the calculated COD values with the experimental measurements of Cowan and Langford (1969).

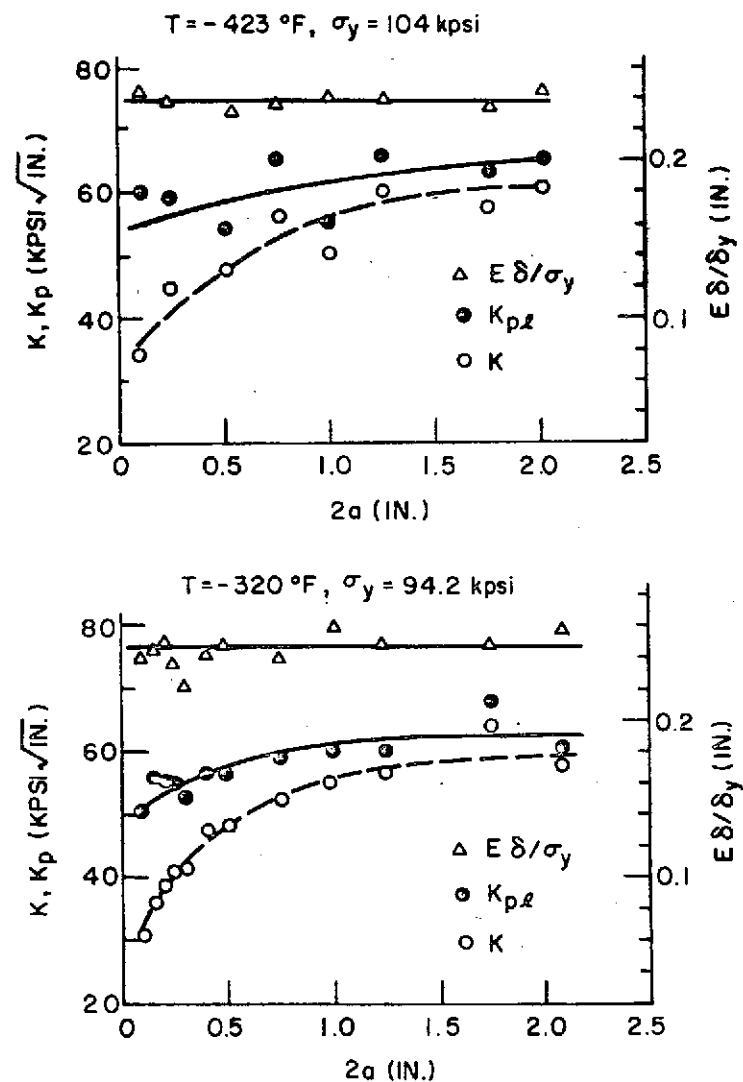


Fig. 12. The results of the burst tests in 2014-T6 aluminum cylinders, $R = 2.81 \text{ in.}$, $h = 0.06 \text{ in.}$ (Anderson and Sullivan, 1966).

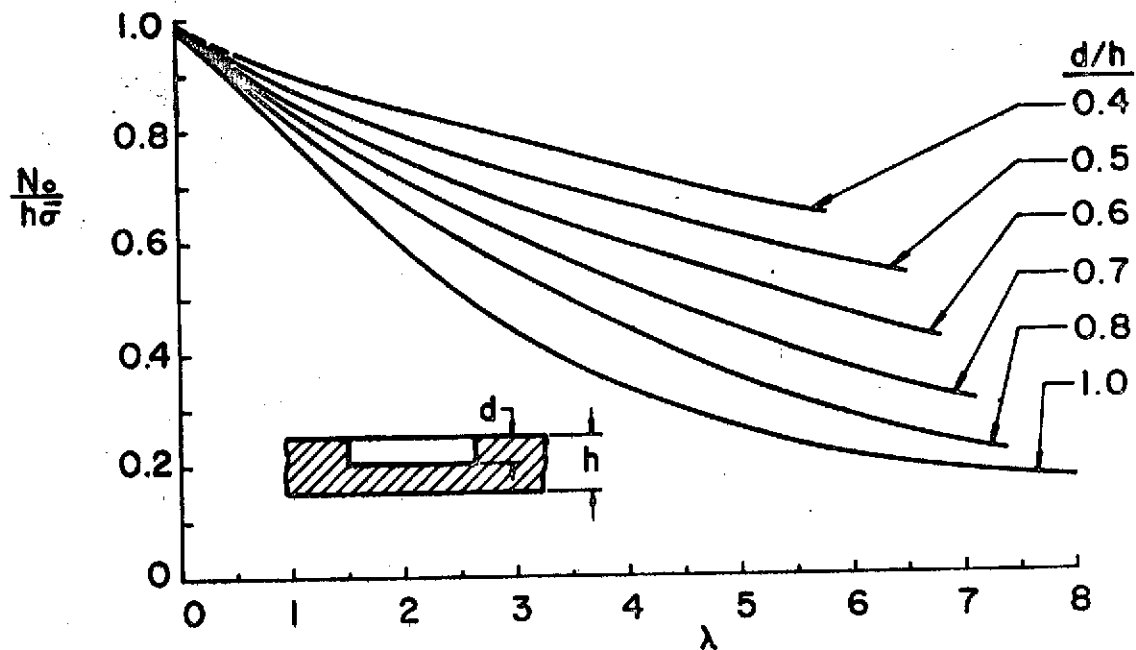


Fig. 13. Load carrying capacity of pressurized cylindrical shells with a part-through or through crack based on the plastic instability criterion.

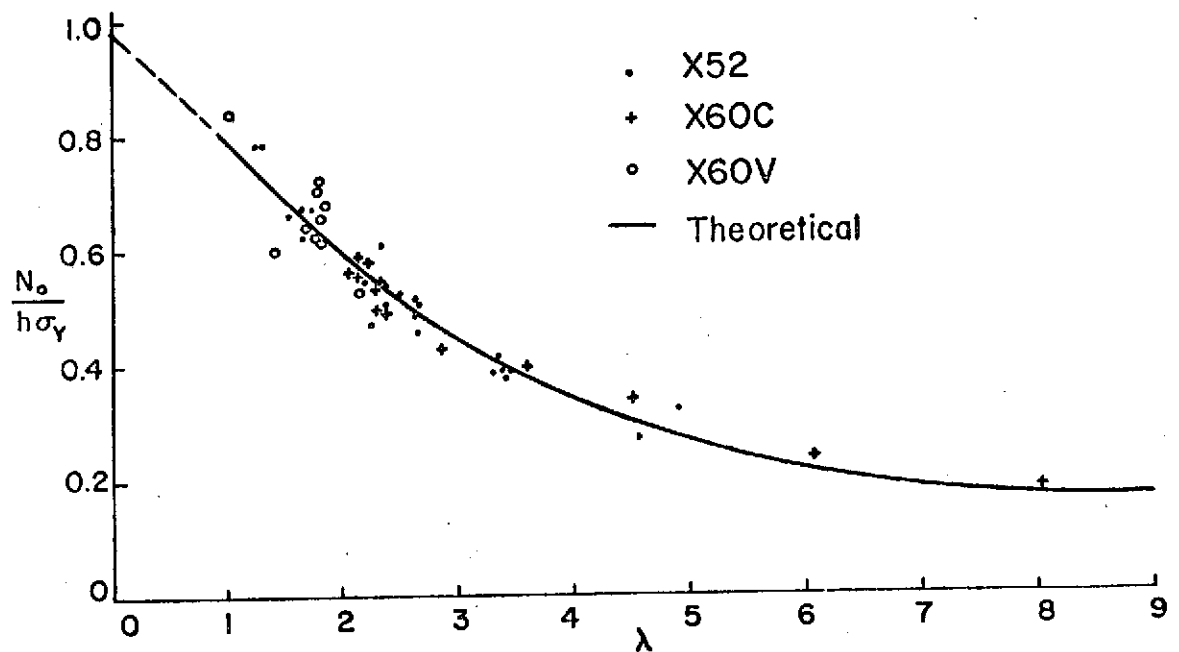


Fig. 14. Comparison of the results of the fracture tests in steel pipes with a through crack (Kiefner, et al. 1972) with that given by the plastic instability criterion.

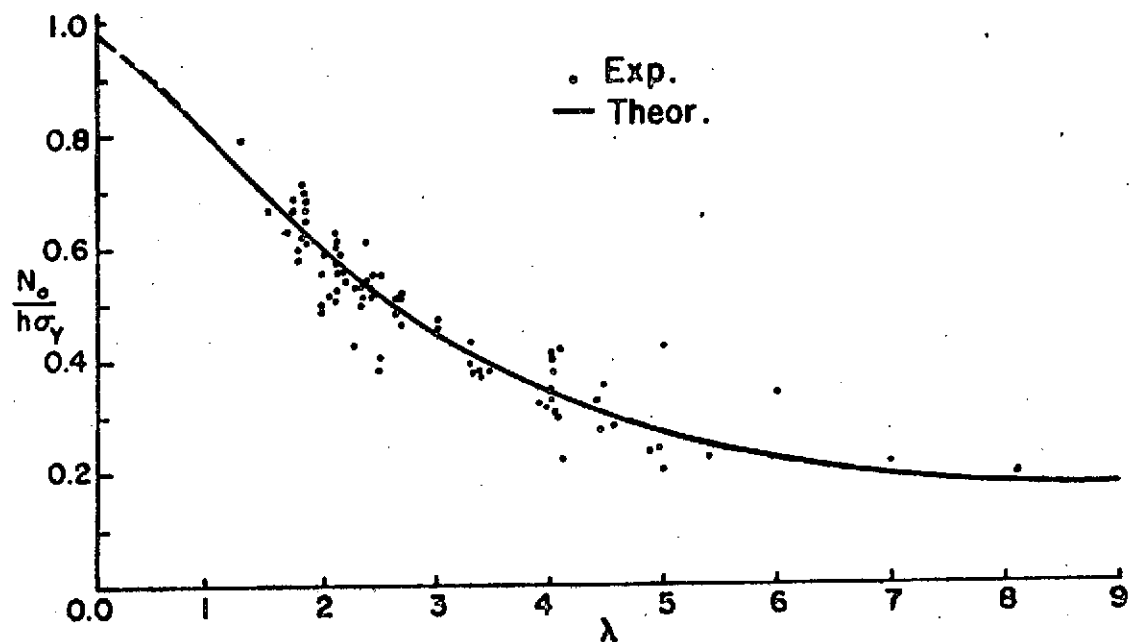


Fig. 15. Same as Fig. 14 for all steel pipes tested by Kiefner, et al. (1972).

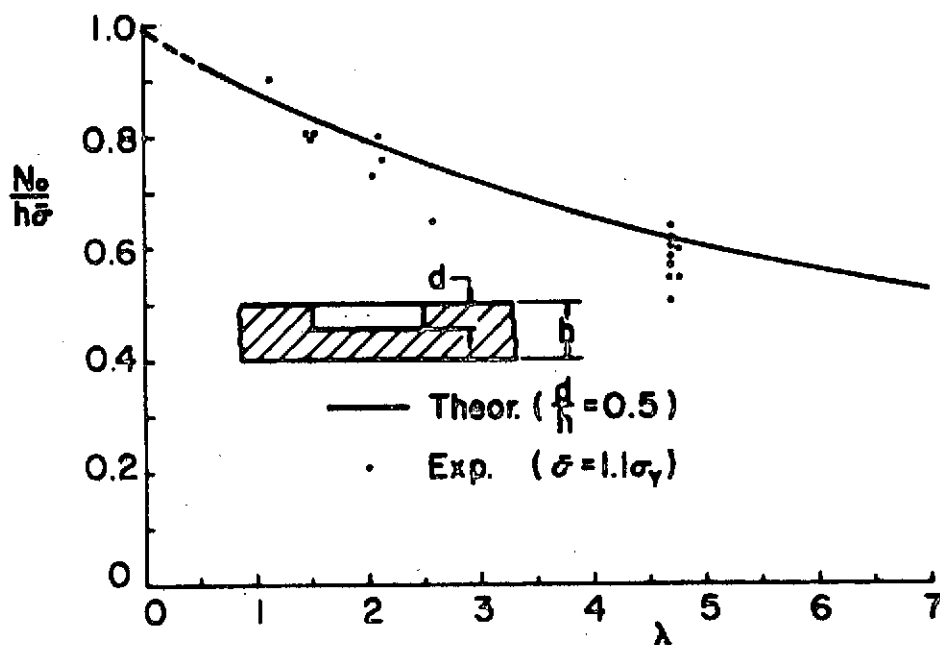


Fig. 16. The results of the fracture tests in steel pipes with a part-through crack, $0.492 < d/h < 0.511$, $\bar{\sigma} = 1.1\sigma_Y$ (Kiefner, et al. 1972). Solid line is the result predicted by fracture instability for $d/h = 0.5$.

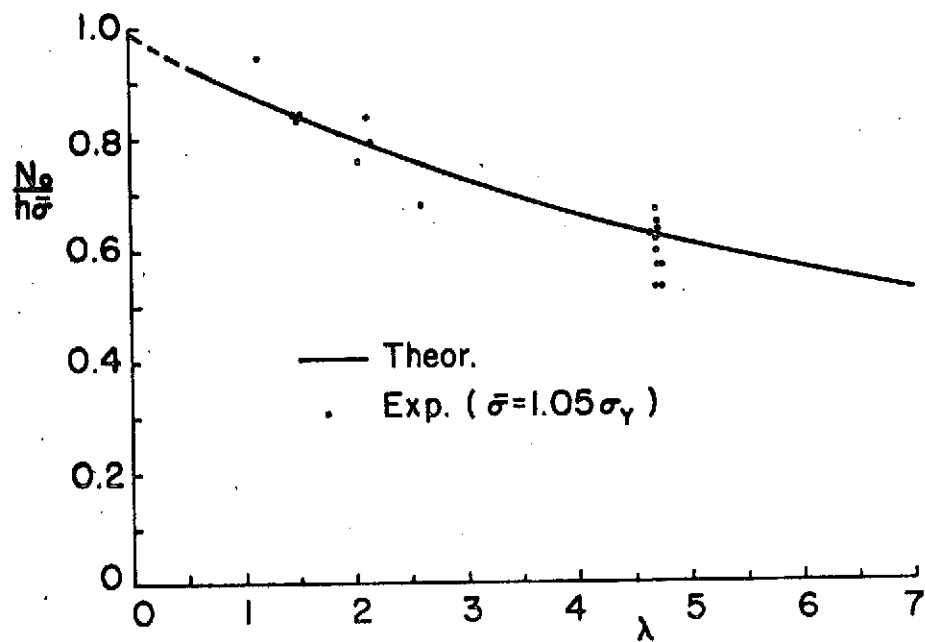


Fig. 17. Same results as in Fig. 16 except the flow stress which is $\bar{\sigma} = 1.05\sigma_Y$.

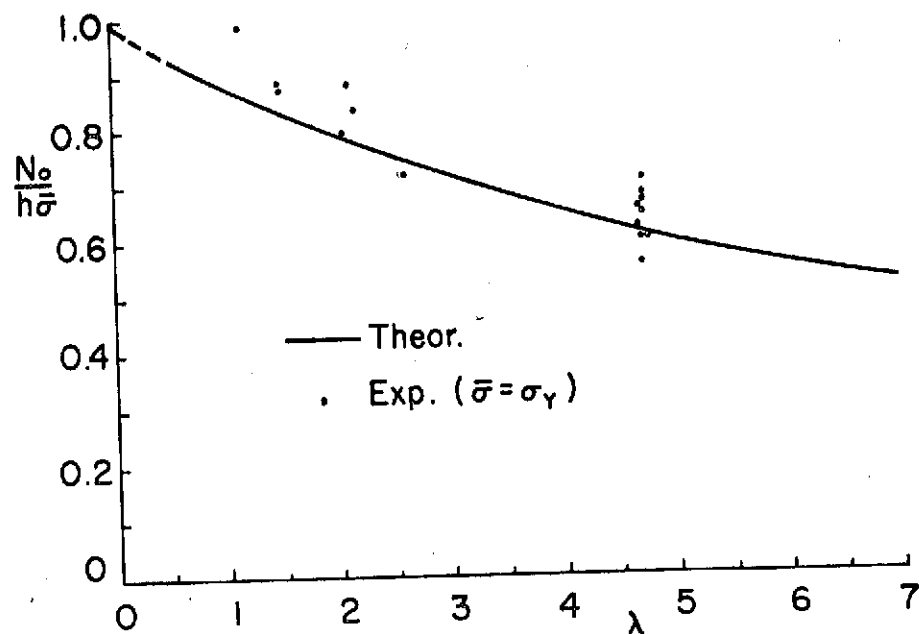


Fig. 18. Same results as in Fig. 16 except the flow stress which is $\bar{\sigma} = \sigma_Y$.

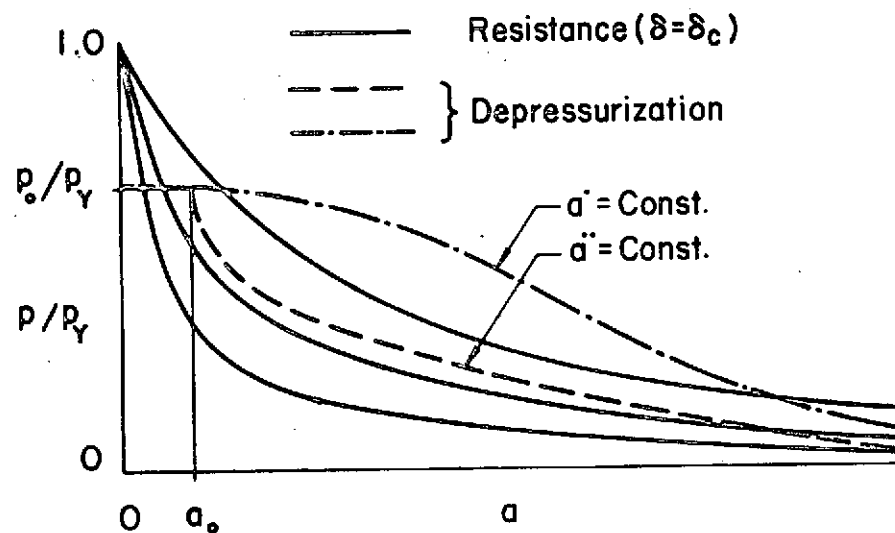


Fig. 19. Qualitative nature of the fracture resistance ($\delta = \delta_c$), and constant velocity and constant acceleration depressurization curves. $2a_0$: initial length of the surface flaw; p_0 : initial pressure.

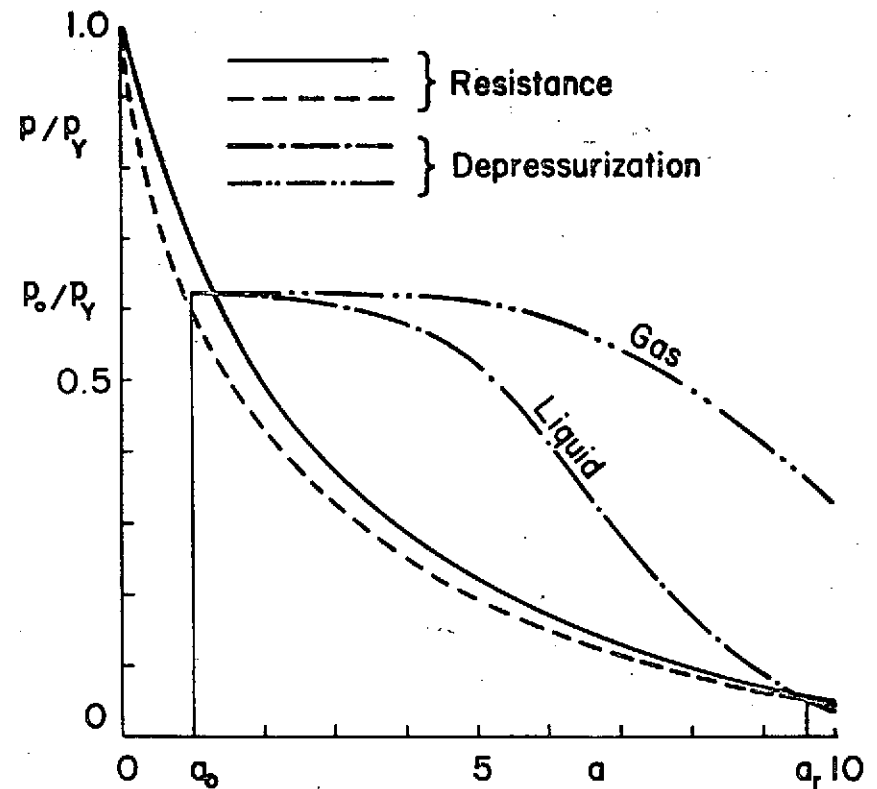


Fig. 20. Pressure vs. crack length corresponding to a constant crack opening stretch $\delta = \delta_c (= 2d_1)$ at the crack tip (the resistance curves), and liquid and gas depressurization curves in a finite-volume cylindrical container with a propagating through crack.